


Circular RNA DENND4C Regulates Cell Malignant Behaviors in Breast Cancer Through the miR-26a-5p/HSPA8 Axis

MeiYan Guo^{1,*}, Yan Chang^{1,*}, YuNa Dai¹, Xia Liu², SuFang Shi¹, JuMei Li¹, WeiGuang Liu³, JianJun Han¹ 

¹Department of Breast Surgery, Affiliated Hospital of Hebei Engineering University, Handan City, Hebei Province, 056002, People's Republic of China;

²Department of Health Examination, Affiliated Hospital of Hebei Engineering University, Handan City, Hebei Province, 056002, People's Republic of China;

³Department of Breast Surgery, Yangzhou Maternal and Child Health Hospital, Yangzhou City, Jiangsu Province, 225007, People's Republic of China

*These authors contributed equally to this work

Correspondence: JianJun Han, Department of Breast Surgery, Affiliated Hospital of Hebei Engineering University, No. 81, Congtai Road, Congtai District, Handan City, Hebei Province, 056002, People's Republic of China, Email hanjianjunHJJ@outlook.com

Objective: At present, the potential functions of most circRNAs in breast cancer (BC) have not been fully elucidated. The investigatory research planned to study biological function of circDENND4C in BC and reveal its downstream molecular mechanism.

Methods: A total of fifty pairs of BC tissue and their corresponding normal tissue were obtained. circDENND4C/miR-26a-5p/Human 71 kDa heat shock cognate protein (HSPA8) were assessed through RT-qPCR or Western blot. After transfecting the relevant plasmids, MKN-45 cell proliferation, cell cycle, invasion, and migration were assessed through MTT and colony formation assays, flow cytometry, and Transwell tests. Bioinformatics analysis, RIP and dual luciferase reporting experiments verified the interaction between circDENND4C, miR-26a-5p, and HSPA8.

Results: Increased circDENND4C was found in BC and was related to a poor prognosis in BC patients. HSPA8 was upregulated and miR-26a-5p was downregulated in BC. Functionally, silencing circDENND4C prevented cells from proliferation, invasion, and migration, and induced cell cycle arrest at G0/G1 phase. circDENND4C overexpression had the opposite effect. The effects of circDENND4C overexpression or knockdown in BC cells were counteracted by overexpressing miR-26a-5p or HSPA8, respectively. circDENND4C mediated HSPA8 expression by competitively adsorbing miR-26a-5p.

Conclusion: circDENND4C absorbs miR-26a-5p to target HSPA8, thereby promoting BC progression, which provides a new insight into the mechanism of BC.

Keywords: circDENND4C, breast cancer, miR-26a-5p, HSPA8

Introduction

Breast cancer (BC), a malignant tumor, typically emerges in the mammary epithelial tissue and contributes to a growing death toll.¹ According to the Globocan (<https://gco.iarc.fr/today>), about 2.26 million people were diagnosed with BC, and 690,000 people died of BC in 2020. Even with improvements in the clinical management of BC, the 5-year overall survival rate is still less than ideal due to tumor high heterogeneity and great differences in clinical outcomes.² Therefore, exploring the molecular mechanism of BC is pivotal for the clinical diagnosis and treatment of BC.

In eukaryotic cells, circRNA is a result of pre-mRNA reverse splicing and is present in both the nucleus and cytoplasm.³ CircRNA has high conservation, stability, and specific expression related to cancer progression and prognosis,^{4,5} making it a biological target for cancer diagnosis and treatment.^{5,6} CircRNAs are increasingly recognized for their involvement in BC progression regulation. Specifically, hsa_circ_0005273 is overexpressed in BC and advances its progression through the regulation of the Hippo signaling pathway.⁷ High levels of circWAC are found in triple negative breast cancer (TNBC), contributing to chemotherapy resistance and resulting in a poor prognosis for patients.⁸

Researchers recently identified that the novel circRNA circDENND4C is expressed abnormally in cancer. Lung cancer proliferation and metastasis are driven by circDENND4C via the enhancement of the bromodomain-containing protein 4 signaling pathway.⁹ circDENND4C is also engaged in managing BC cell proliferation, invasion, migration, and glycolysis during hypoxia.^{10,11} However, it is not clear whether circDENND4C has a similar effect on BC cells in the normoxic environment.

In tumors, abnormally expressed circRNA functions as a ceRNA for miRNA, modulating target gene expression and affecting the progression of tumors.^{12–14} For example, hsa_circ_0025202 regulates miR-182-5p to exert anti-tumor effects on hormone receptor-positive BC.¹⁵ The interaction of circCD44 and miR-502-5p accelerates TNBC tumorigenesis.¹⁶ Based on this, the study analyzed and screened the potential miRNA and target mRNA of circDENND4C, miR-26a-5p, and human 71 kDa heat shock cognate protein (HSPA8), through the starBase database. miR-26a-5p has been considered to be associated with autophagy in BC.¹⁷ HSPA8, found on chromosome 11q23.3, is part of the HSP70 protein family and holds importance in autophagy decision processes.^{18,19}

This study aimed to clarify the biological functions of circDENND4C in BC cells and map out the related downstream miRNA/mRNA signaling pathways. A combination of molecular biological and bioinformatics techniques confirmed the interactions among circDENND4C, miR-26a-5p, and HSPA8 in the context of BC. Furthermore, the regulatory mechanisms of these molecules on BC proliferation, invasion, migration, and cell cycle were explored.

Materials and Methods

Clinical Sample Acquisition

From May 2015 to March 2017, tumor tissues and matched non-tumor tissues (located >3 cm from the tumor margin) were surgically excised from 50 patients diagnosed with primary BC at the Affiliated Hospital of Hebei Engineering University. None of the patients had received preoperative chemotherapy, radiotherapy, or endocrine therapy. Of these patients, 32 were hormone receptor-positive, 11 were HER2-positive, and 7 had TNBC. The patient's clinical information is available in the [Supplementary Table](#). Postoperative pathological examinations confirmed the absence of cancer cells in the non-tumor tissues. Immediately after collection, all specimens were snap-frozen in liquid nitrogen and stored at -80°C for extracting RNA. All 50 patients were followed up via telephone and medical record review until March 2022, with a median follow-up duration of 60 months. The study was approved by the Ethics Committee of the Affiliated Hospital of Hebei Engineering University (Ethics approval number: 20141211HBEU), and written informed consent was obtained from all participants.

Survival Analysis

Survival analysis utilized circDENND4C expression data along with clinical follow-up details from a cohort of 50 patients as detailed in this study. Based on circDENND4C's median expression level, patients were categorized into groups with high and low expression levels. The Kaplan-Meier method was employed to create comprehensive survival graphs, with the log-rank (Mantel-Cox) test assessing the statistical relevance of the curve differences.

Cell Culture

The human BC cell lines BT-549, MDA-MB-231, MDA-MB-468, MCF-7, T-47D, and SKBR-3, as well as the normal mammary epithelial cell line MCF-10A, were purchased from the American Type Culture Collection (USA). BC cell lines were cultured in Dulbecco's modified Eagle medium (DMEM) from Gibco, USA, with the addition of 10% fetal bovine serum (FBS) and 1% penicillin-streptomycin (50 U/mL), both from Gibco. MCF-10A cells were grown in DMEM/F-12 medium (Gibco) supplemented with its requisite growth factors. Every cell underwent cultivation in a moisture-controlled incubator (Thermo Fisher Scientific, USA), maintained at 37°C and containing 5% CO_2 . All cells used in the experiments were limited to 10 passages to ensure consistent phenotypes and reproducible results.

Actinomycin D Experiment

MCF-7 cells were grown in 6-well plates, and when they achieved 90–100% confluence, the medium was replaced with fresh DMEM with 2 µg/mL actinomycin D (KE1084, Kingmorn, Shanghai, China). Cells were harvested at 0, 4, 8, and 12 h following treatment. Total RNA was then extracted to determine circDENND4C and the linear GAPDH and β-actin mRNA by RT-qPCR.

RT-qPCR

Total RNA was extracted from tissues and cells using TRIzol reagent (Invitrogen, USA). After determining RNA concentration and purity using a NanoDrop spectrophotometer, 1 µg of total RNA was transcribed into cDNA with the PrimeScript™ RT kit (Invitrogen). The procedure for RT-qPCR involved the Bio-Rad CFX96 quantitative PCR system along with SYBR Green Real-Time PCR Master Mixes (Thermo Fisher Scientific). Internal controls for mRNA/circRNA and miRNA were GAPDH and U6 small nuclear RNA, respectively. The stability of GAPDH and U6 as reference genes was validated across the experimental groups, confirming that their expression levels remained constant (standard deviation of Ct values < 0.5). The relative gene expression was calculated using the $2^{-\Delta\Delta Ct}$ method. All primer sequences are presented in Table 1.

Cell Transfection

The small interfering RNA targeting circDENND4C (si-circDENND4C; target sequence: 5'-GACATTGCCATTATTATCAAA-3'), a non-targeting control siRNA (si-NC), miR-26a-5p mimic, and mimic negative control (mimic NC) were synthesized by Ibsbio (Shanghai, China). The pcDNA3.1 overexpression vectors for circDENND4C and HSPA8, along with the empty pcDNA3.1 vector, were also obtained from Ibsbio. For rescue experiments, a siRNA-resistant circDENND4C expression vector (pcDNA3.1-circDENND4C-Res) was constructed by introducing point mutations into the siRNA target site (sequence mutated from 5'-GACATTGCCATTATTATCAAA-3' to 5'-GATATCGCAATCATCATAAAG-3'), rendering its transcript immune to degradation by si-circDENND4C. MCF-7 cells were seeded in 6-well plates and grown to 70–80% confluence before being transiently transfected using HieffTrans™ liposomal transfection reagent (Yeasten, Shanghai, China). At 48 h post-transfection, transfection efficiency was verified by RT-qPCR or immunoblotting, and cells were harvested for subsequent functional assays.

3-(4,5-Dimethylthiazol-2-Yl)-2,5-Diphenyltetrazolium Bromide (MTT) Test

During the logarithmic growth stage, cells were planted in 96-well plates, maintaining 1×10^4 cells/well. At 24, 48, and 72 h, each well received 20 µL of MTT solution (5 mg/mL) and was kept at 37°C for 4 h. The supernatant was then

Table 1 PCR Primer Sequences

| | Primer Sequences (5' - 3') |
|-------------|--------------------------------------|
| circDENND4C | Forward: 5'- GGGAGAGATAAACCACCGCT-3' |
| | Reverse: 5'- CAGTGAGACCAGCTACGACA-3' |
| miR-26a-5p | Forward: 5'- GCGCTTCAAGTAATCCAGGA-3' |
| | Reverse: 5'- TGGTGTCTGGAGTCG-3' |
| HSPA8 | Forward: 5'- GCAATGAACCCCACCAACAC-3' |
| | Reverse: 5'- CTACTTGGACCTTGGGCCTG-3' |
| U6 | Forward: 5'- CTCGCTTCGGCAGCACA-3' |
| | Reverse: 5'- AACGCTTACGAATTTGCGT-3' |
| GAPDH | Forward: 5'- CACCCACTCCTCCACCTTTG-3' |
| | Reverse: 5'- CCACCACCCTGTTGCTGTAG-3' |

discarded, and 150 μ L of dimethyl sulfoxide was introduced into each well to dissolve the formazan crystals. Using a microplate reader, the optical density (OD) was gauged at 490 nm.

Clonal Formation Experiment

The transfected MCF-7 cells were distributed into six-well plates, maintaining a concentration of 800 cells in each well. Cultivation of the cells spanned roughly 10 days, during which the entire medium was refreshed every three days. The formed colonies underwent two PBS washes, were stabilized using 4% paraformaldehyde for 10 min and colored with a 0.5% crystal violet mixture for 15 min. Following a triple rinse with ddH₂O, the plates underwent photography, and the colonies were tallied.

Cell Cycle Detection

Transfected MCF-7 cells were washed twice with ice-cold PBS, fixed in ice-cold 75% ethanol at 4°C overnight, and stained with a propidium iodide (PI)/RNase A staining solution (Beyotime, Shanghai, China) for 30 min at 37°C in the dark. Cell cycle distribution analysis was conducted using a flow cytometer (BD Pharmingen).

Transwell Experiment

Cell migration and invasion assays utilized 24-well Transwell chambers (Corning, USA) with an 8- μ m pore size. The invasion test involved coating the upper chamber with Matrigel (BD Biosciences, catalog number 356234). In the upper chamber, 5×10^4 cells resuspended in serum-free DMEM were added, while the lower chamber contained 600 μ L of DMEM with 10% FBS. Cells transfected with si-NC or an empty vector made up the control groups. After incubating for 24 h, non-migrating and non-invading cells on the upper surface were wiped away with a cotton swab. After migrating or invading to the lower surface, cells were fixed with 4% paraformaldehyde for 10 min, stained with 0.5% crystal violet, and counted under an inverted microscope in 5 random areas.

Immunoblotting

Total protein extraction from tissues and cells was performed using RIPA lysis buffer enriched with protease inhibitor mixture (Roche). Proteins were measured utilizing the bicinchoninic acid Protein Assay Kit (Pierce, 23227). Identical quantities of protein (20 μ g) underwent separation through 10% sodium dodecyl sulfate-polyacrylamide gel electrophoresis and were then moved onto polyvinylidene difluoride membranes. Membranes were blocked with a mixture of 5% non-fat milk in Tris-buffered saline and 0.1% Tween 20 for 1 h, followed by an overnight incubation with primary antibodies at 4°C. Utilized primary antibodies included GAPDH (ab8245, Abcam, 1:10000) and HSPA8 (#8444, Cell Signaling Technology, 1:1000). The membranes were treated with a goat anti-rabbit HRP-linked secondary antibody (1:3000) for 1 h. The visualization of protein bands was achieved through the application of an enhanced chemiluminescence (ECL) detection system (Thermal Fisher Scientific).

Luciferase Reporter Assay

Specific fragments of circDENND4C and HSPA8 3'-UTR, which include the anticipated binding site of miR-26a-5p, were integrated into the psiCHECK2 vector (Ibsbio) and designated as circDENND4C-WT and HSPA8-WT. Furthermore, the creation of circDENND4C-MUT and HSPA8-MUT luciferase reporter vectors was accomplished. Using HieffTransTM liposomes, the reporter vector along with miR-26a-5p mimic or mimic NC were jointly introduced into MCF-7 cells and their luciferase activities were examined with the Dual-LumiTM Luciferase Reporter Gene Assay Kit (Beyotime). The firefly activity was standardized against the renilla signal, and presented as the ratio of firefly to renilla activity.

RNA Immunoprecipitation (RIP) Experiment

The Magna RIPTM RNA-Binding Protein Immunoprecipitation Kit (Millipore, USA), was utilized for performing RIP assays. Briefly, approximately 1×10^7 MCF-7 cells were collected and lysed in 1 mL of complete RIP lysis buffer. The cell lysate was centrifuged, and 2 mg of total protein from the supernatant was incubated overnight at 4°C with magnetic

beads pre-coated with 5 μ g of anti-Ago2 antibody (Abcam) or control rabbit IgG. The day after, the beads were collected using a magnetic rack and washed six times with cold RIP Wash Buffer. The RNA-protein complexes were then eluted, and RNA was purified after undergoing proteinase K digestion. The enrichment of circDENND4C and miR-26a-5p was analyzed by RT-qPCR.

Data Analysis

The experiments were carried out in sets of three, with the data displayed as the mean \pm standard deviation (SD). Statistical analyses were conducted using GraphPad Prism 9.0. To assess differences between two groups, an unpaired two-tailed Student's *t*-test was conducted, and for multiple groups, a one-way ANOVA with a subsequent Tukey's post hoc test was performed. Statistical significance was assigned to *P*-values below 0.05.

Results

Abundance of circDENND4C Expression in BC

First, circDENND4C expression pattern was evaluated by RT-qPCR in BC. circDENND4C expression was higher in BC tissues than that in non-tumor tissues (Figure 1A), as well as in BC cell lines than that in MCF-10A cells (Figure 1B). The information of circDENND4C was checked on the bioinformatics website circbank, which is 322bp in length and located in chr9:19276155–19276477 strand: + (Figure 1C). Subsequently, the ring structure of circDENND4C was detected by actinomycin D assay, and it was the stability of GAPDH mRNA affected by actinomycin D, but not that of circDENND4C (Figure 1D). Subsequently, the association between circDENND4C and 5-year survival in BC patients was examined, and the Kaplan-Meier analysis revealed that BC patients exhibiting elevated circDENND4C levels

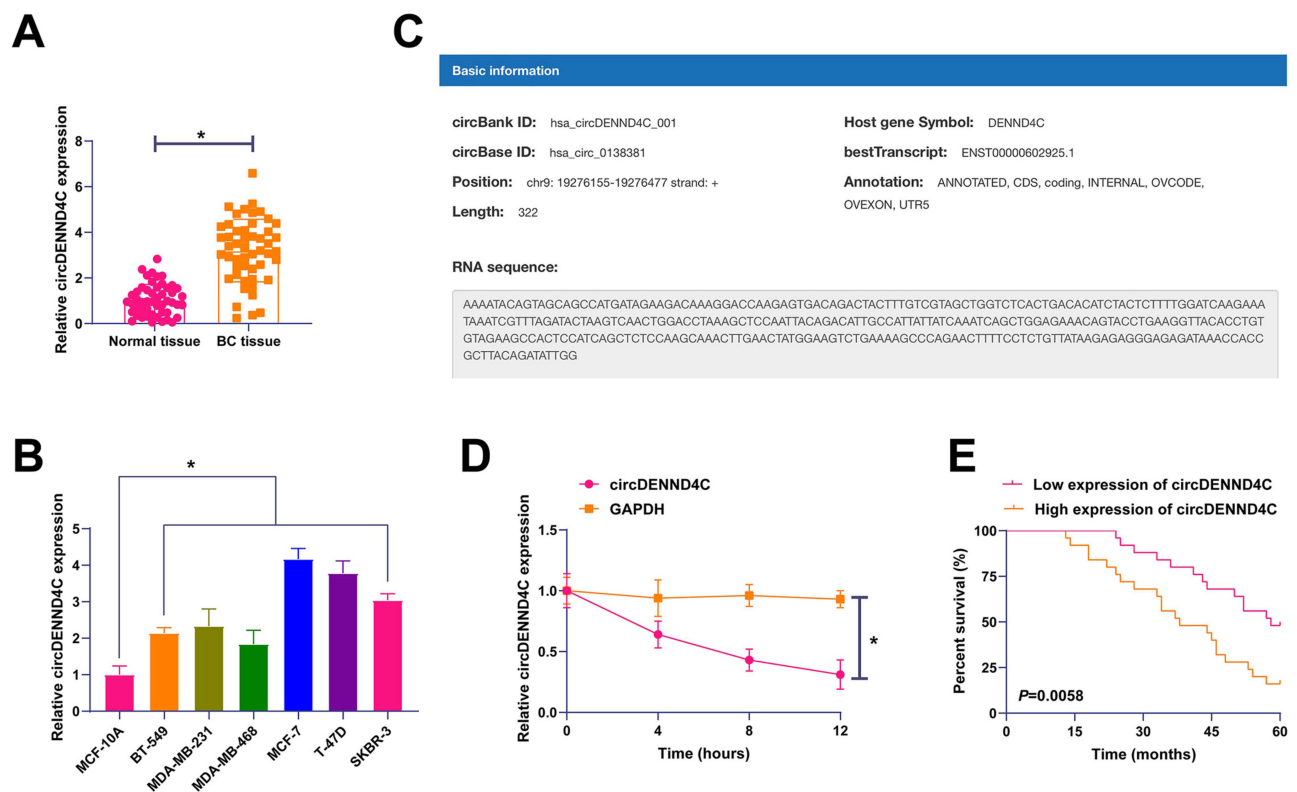


Figure 1 circDENND4C is upregulated in breast cancer and associated with poor prognosis. (A) RT-qPCR analysis shows significantly higher expression of circDENND4C in BC tissues compared to adjacent normal tissues (n=50). (B) RT-qPCR analysis of circDENND4C expression across a panel of six BC cell lines and the normal mammary epithelial cell line MCF-10A. (C) A schematic diagram from the circBank database illustrating the genomic location and back-splicing of circDENND4C from the DENND4C gene. (D) The stability of circDENND4C was assessed in MCF-7 cells treated with actinomycin D. RT-qPCR results demonstrate that circDENND4C is substantially more stable than the linear GAPDH mRNA. (E) Kaplan-Meier survival analysis of 50 BC patients indicates that high circDENND4C expression is correlated with a lower 5-year overall survival rate (Log rank test). Data are expressed as mean \pm SD (N = 3). **P* < 0.05.

experienced a reduced five-year survival rate (Figure 1E). The findings indicate high expression of circDENND4C in BC, potentially playing a role in its development.

circDENND4C Promotes Malignant Phenotypes in BC

To investigate the biological function of circDENND4C in breast cancer, we first performed loss-of-function experiments in MCF-7 cells, which exhibit relatively high endogenous expression of circDENND4C. We designed and transfected a specific small interfering RNA (si-circDENND4C) to deplete circDENND4C. RT-qPCR analysis confirmed that si-circDENND4C significantly reduced the expression of circDENND4C compared to the non-targeting control (si-NC) group (Figure 2A). circDENND4C knockdown was shown to inhibit the proliferation and colony-forming capacity of MCF-7 cells through MTT and colony formation assays (Figure 2B and C). Furthermore, flow cytometry analysis demonstrated that circDENND4C knockdown led to cell cycle arrest at the G0/G1 phase, as indicated by an increased number of cells in this phase and a corresponding reduction in the S phase population (Figure 2D). Transwell assays also showed that silencing circDENND4C significantly impaired the migratory and invasive capabilities of MCF-7 cells (Figure 2E). To ensure that these observed phenotypes were specifically due to the depletion of circDENND4C and not off-target effects of the siRNA, we conducted a rescue experiment. We engineered a circDENND4C expression vector (circDENND4C-Res) containing silent mutations in the siRNA target sequence, rendering it resistant to si-circDENND4C-mediated degradation. As shown by RT-qPCR, co-transfection of circDENND4C-Res with si-circDENND4C successfully restored circDENND4C expression to levels comparable to the control group (Figure 2A). The re-expression of this resistant circDENND4C construct reversed the siRNA's inhibitory effects on cell phenotypes as indicated above (Figure 2B–E). Collectively, these findings strongly indicate that circDENND4C acts as a potent oncogene in breast cancer.

MiR-26a-5p is Bound to circDENND4C in BC

Subsequently, the possible miRNAs that bind to circDENND4C were examined. The bioinformatics website starbase forecasted possible binding sites between miR-26a-5p and circDENND4C (Figure 3A). Co-transfection of the miR-26a-

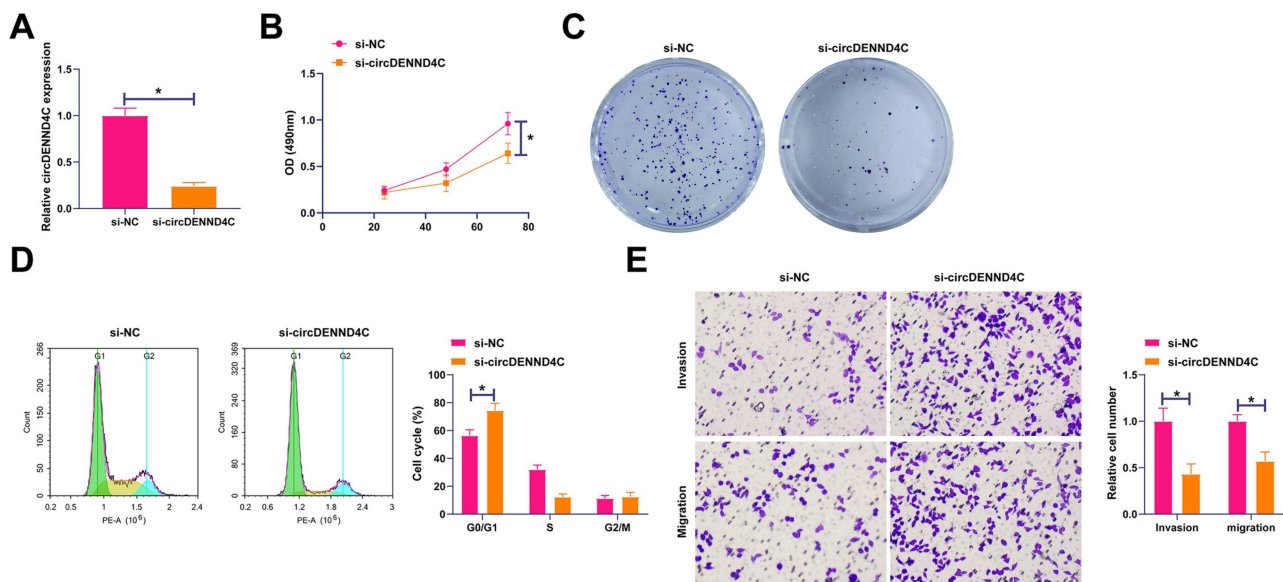


Figure 2 Knockdown of circDENND4C inhibits malignant behaviors of BC cells, an effect rescued by an siRNA-resistant construct. MCF-7 cells were transfected with a non-targeting control siRNA (si-NC), a siRNA targeting circDENND4C (si-circDENND4C), or co-transfected with si-circDENND4C and a resistant circDENND4C expression vector (circDENND4C-Res). (A) RT-qPCR was used to confirm the successful knockdown of circDENND4C by its siRNA and its effective restoration by the circDENND4C-Res vector. (B and C) MTT (B) and colony formation (C) assays demonstrate that circDENND4C knockdown suppressed cell proliferation, while re-expression of the resistant circDENND4C rescued this inhibitory effect. (D) Flow cytometry analysis of the cell cycle shows that circDENND4C depletion induced G0/G1 phase arrest, which was reversed upon co-transfection with circDENND4C-Res. (E) Transwell assays reveal that the inhibition of cell migration and invasion caused by circDENND4C knockdown was significantly rescued by the expression of circDENND4C-Res. Data are expressed as mean \pm SD (N = 3). *P < 0.05.

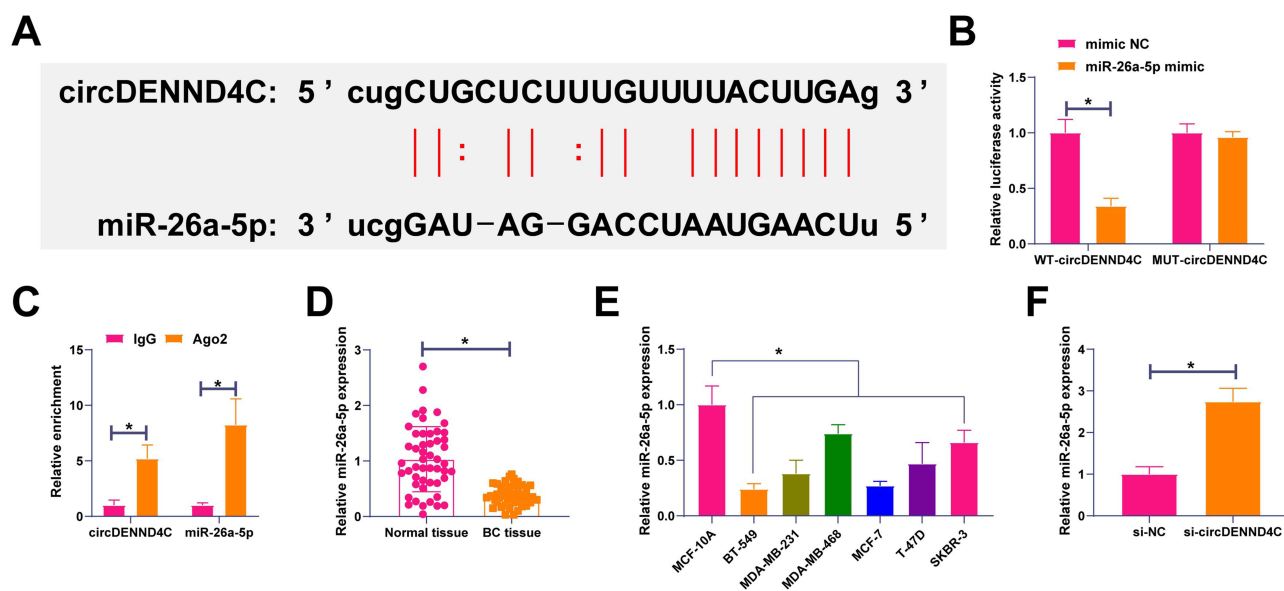


Figure 3 circDENND4C directly binds to and sponges miR-26a-5p in BC. **(A)** The predicted binding site between circDENND4C and miR-26a-5p from the starBase database. The mutant sequence for the luciferase assay is also shown. **(B)** Dual-luciferase reporter assay in MCF-7 cells. Co-transfection of miR-26a-5p mimic with the circDENND4C-WT reporter significantly reduced luciferase activity, whereas this effect was abolished in the circDENND4C-MUT reporter. **(C)** RNA immunoprecipitation (RIP) assay using an anti-Ago2 antibody in MCF-7 cells demonstrates significant enrichment of both circDENND4C and miR-26a-5p compared to the IgG control. **(D and E)** RT-qPCR analysis shows that miR-26a-5p is downregulated in BC tissues **(D)** and cell lines **(E)** compared to their respective controls. **(F)** Knockdown of circDENND4C in MCF-7 cells led to a significant increase in miR-26a-5p expression. Data are expressed as mean \pm SD (N = 3). *P < 0.05.

5p mimic with the circDENND4C-WT reporter vector led to a significant suppression of luciferase activity in MCF-7 cells compared to the mimic control group. In stark contrast, this inhibitory effect was completely abolished when the miR-26a-5p mimic was co-transfected with the circDENND4C-MUT vector, whose luciferase activity remained unchanged (Figure 3B). This result directly demonstrates that the interaction is dependent on the predicted binding sequence. Furthermore, an RIP assay using an anti-Ago2 antibody confirmed the significant co-enrichment of both circDENND4C and miR-26a-5p in the Ago2-containing complex, further supporting their interaction within the RNA-induced silencing complex (Figure 3C). Afterward, miR-26a-5p expression in BC was analyzed, showing that its levels were lower in BC tissues and cell lines than in non-tumor tissues or cell lines (Figure 3D and E). Following this, the study focused on how circDENND4C regulates miR-26a-5p, revealing that reducing circDENND4C elevated miR-26a-5p expression in MCF-7 cells (Figure 3F). The findings indicate that circDENND4C forms a competitive bond with miR-26a-5p.

MiR-26a-5p Participates in circDENND4C Regulating BC Malignant Behaviors

The interaction between circDENND4C and miR-26a-5p in BC was explored through functional rescue experiments. MCF-7 cells were co-transfected with pcDNA 3.1-circDENND4C and miR-26a-5p mimic. pcDNA 3.1-circDENND4C up-regulated circDENND4C and decreased miR-26a-5p, while miR-26a-5p mimic restored miR-26a-5p expression (Figure 4A). Functional rescue assays showed that circDENND4C elevation promoted cell proliferation and clonal cell number, reduced the proportion of cells in the G0/G1 phase, and promoted cell invasive and migratory behaviors, but elevating miR-26a-5p could block the above-mentioned influences (Figure 4B–E). These data suggest that circDENND4C affects the malignant behavior of BC by regulating miR-26a-5p.

HSPA8 is Modulated by miR-26a-5p

Starbase identified possible binding sites for HSPA8 and miR-26a-5p (Figure 5A). The assay revealed that co-transfection of the miR-26a-5p mimic with the HSPA8-WT reporter vector resulted in a significant reduction in luciferase activity. Crucially, this suppressive effect was completely abrogated when the binding site was mutated in the HSPA8-MUT reporter, indicating that the binding is sequence-specific (Figure 5B). To further validate this interaction in

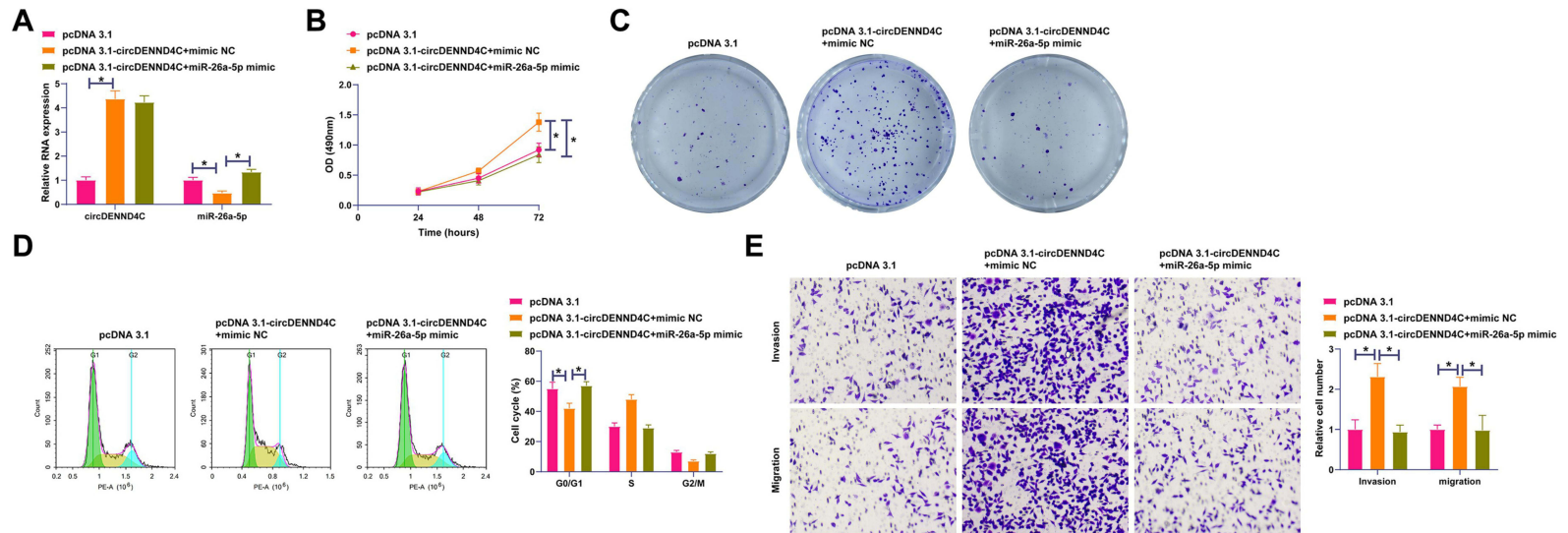


Figure 4 miR-26a-5p overexpression reverses the pro-malignant effects of circDENND4C. MCF-7 cells were co-transfected with a circDENND4C overexpression vector (pcDNA 3.1-circDENND4C) and a miR-26a-5p mimic or their respective controls. **(A)** RT-qPCR validation of circDENND4C overexpression and the restoration of miR-26a-5p levels by its mimic. **(B and C)** The promotion of cell proliferation by circDENND4C overexpression, as shown by MTT **(B)** and colony formation **(C)** assays, was counteracted by co-transfection with miR-26a-5p mimic. **(D)** Overexpression of circDENND4C promoted G1/S phase transition, an effect that was blocked by elevating miR-26a-5p levels. **(E)** Transwell assays show that the enhanced migration and invasion abilities induced by circDENND4C were reversed by the miR-26a-5p mimic. Data are expressed as mean \pm SD (N = 3). *P < 0.05.

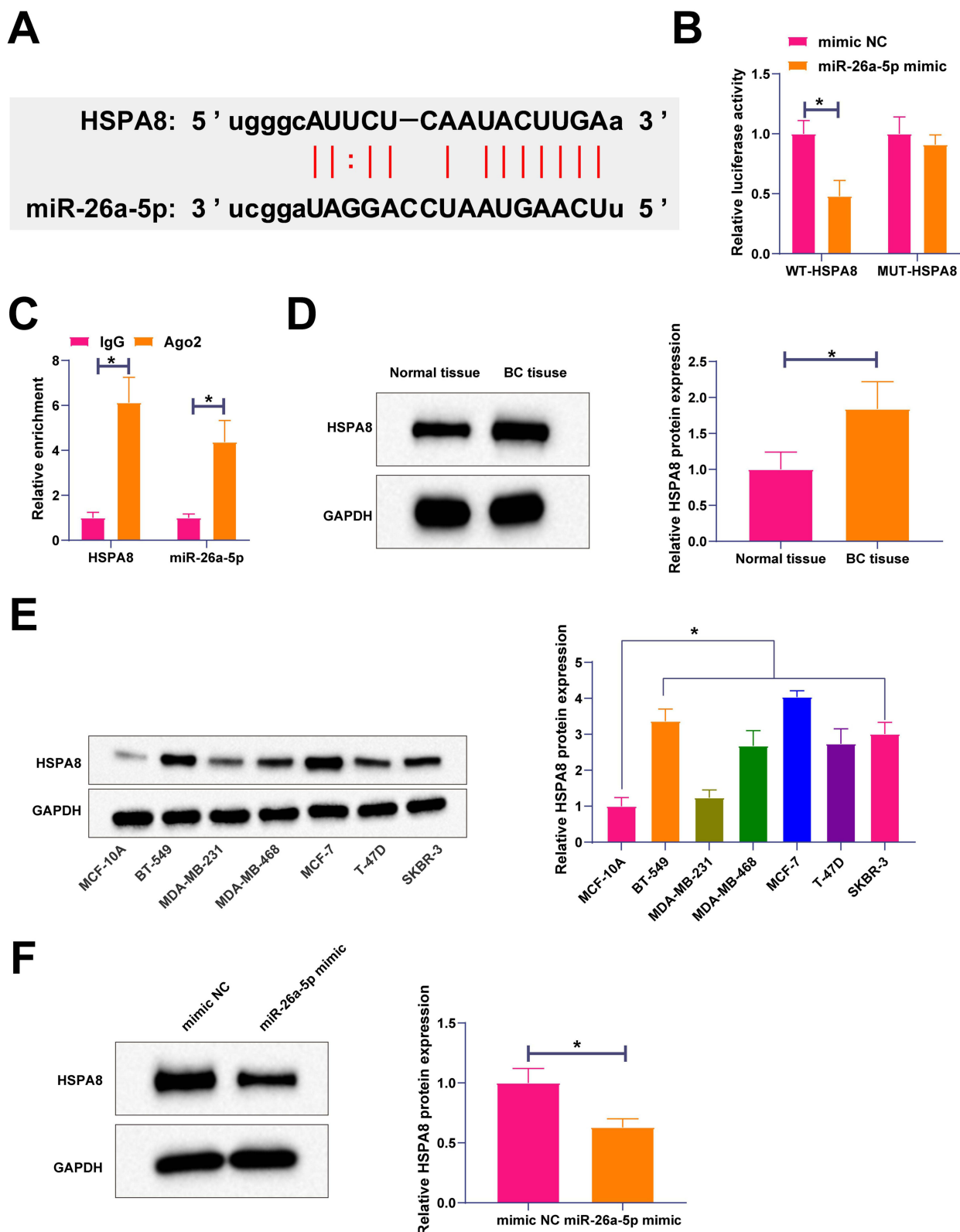


Figure 5 HSPA8 is a direct target of miR-26a-5p and is upregulated in BC. **(A)** Prediction of the miR-26a-5p binding site in the 3'-UTR of HSPA8 from the starBase database, with the mutant sequence indicated. **(B)** Dual-luciferase reporter assay shows that miR-26a-5p mimic suppressed the luciferase activity of the HSPA8-WT reporter but not the HSPA8-MUT reporter in MCF-7 cells. **(C)** RIP assay with an anti-Ago2 antibody confirms the co-enrichment of HSPA8 mRNA and miR-26a-5p in MCF-7 cells. **(D and E)** Western blot analysis reveals that HSPA8 protein expression is elevated in BC tissues **(D)** and cell lines **(E)** compared to controls. **(F)** Overexpression of miR-26a-5p in MCF-7 cells resulted in a marked decrease in HSPA8 protein levels. Data are expressed as mean \pm SD (N = 3). *P < 0.05.

a physiological context, an anti-Ago2 RIP assay was performed, which confirmed that both HSPA8 mRNA and miR-26a-5p were significantly enriched in the Ago2-immunoprecipitated fraction (Figure 5C). Subsequently, the expression pattern of HSPA8 in BC was analyzed by Western blot. High levels of HSPA8 were found in BC tissues and cell lines (Figure 5D and E), and miR-26a-5p overexpression weakened HSPA8 expression in MCF-7 cells (Figure 5F). The evidence pointed to HSPA8 being a downstream target of miR-26a-5p.

HSPA8 Participates in circDENND4C Regulating BC Malignant Behaviors

A functional rescue experiment was conducted to explore whether HSPA8 was involved in the process of circDENND4C regulating BC. si-circDENND4C and pcDNA 3.1-HSPA8 were co-transfected into MCF-7 cells. Figure 6A confirms that the prohibitive effect of si-circDENND4C on HSPA8 expression was recovered by pcDNA 3.1-HSPA8. Functional assays further illustrated that knocking down circDENND4C suppressed cell proliferation and cloning, elevated the G0/G1 phase cell ratio, and diminished cell invasion and migration, yet these changes were overturned by HSPA8 overexpression (Figure 6B–E).

Discussion

BC maliciously harms public health, contributing to high morbidity and mortality.²⁰ CircRNAs have been considered keys in human cancer development^{21–23} and can modulate tumor activities.²⁴ This study attempted to explore circDENND4C in BC cells in the normoxic environment, with a view to providing new targets and insights for the clinical treatment of BC. This study summarized that CircDENND4C silencing disrupted BC malignant behaviors by regulating the miR-26a-5p/HSPA8 axis, thus inhibiting the malignant progression of BC.

The biological function of circDENND4C has been investigated in several malignancies, revealing diverse and, in some cases, opposing roles. A body of evidence supports an oncogenic function. circDENND4C contributes to lung cancer cell proliferation and metastasis by activating the BRD4 signaling pathway.²⁵ In colorectal cancer, it facilitates glycolysis and migration via the miR-760/GLUT1 axis,²⁶ while in hepatocellular carcinoma, it activates the Wnt/ β -catenin pathway through the modulation of TCF4.²⁷ These findings establish circDENND4C as a pro-tumorigenic factor in multiple cancer types.

However, the role of circDENND4C appears to be highly dependent on the cellular and microenvironmental context. Within breast cancer, its function is contingent on oxygen availability. Previous studies established that circDENND4C is induced by HIF1 α under hypoxic conditions, where it regulates glycolysis and invasion by targeting the miR-200b/c family.^{11,28} In contrast, our study, conducted under normoxic conditions, delineates a distinct regulatory mechanism involving the miR-26a-5p/HSPA8 axis. This demonstrates that the downstream signaling of circDENND4C is reprogrammed by the tumor microenvironment. Further evidence for its functional plasticity is provided by a study in epithelial ovarian cancer, where circDENND4C was characterized as a tumor suppressor that functions by downregulating miR-200b/c.²⁹ The observation that circDENND4C can function as either an oncogene or a tumor suppressor, while in different contexts targeting the same miRNA family (miR-200b/c), indicates that its biological output is dictated by tissue-specific factors. Therefore, our identification of the oncogenic circDENND4C/miR-26a-5p/HSPA8 axis provides crucial insight into its function within the specific and clinically prevalent context of normoxic breast cancer, contributing to a more complete understanding of this functionally plastic molecule.

CircRNA-miRNA-mRNA regulatory network has attracted academic attention to the pathogenesis and progression of BC. Most circRNAs can function as miRNA sponges to regulate tumor progression by ceRNA mechanisms.^{30,31} miR-26a-5p was screened and studied in the process of circDENND4C regulating BC. miR-26a-5p is underexpressed in tumors, including BC, thyroid cancer, and pancreatic ductal cancer, and is associated with patient's prognosis.^{32–34} Meanwhile, artificially modulating miR-26a-5p is of feasibility to reduce paclitaxel resistance of triple-negative BC cells, thereafter to control tumor growth.¹⁷ The study results highlighted that increasing miR-26a-5p expression weakened circDENND4C overexpression-promoted malignancy of BC cells.

Later, miR-26a-5p targeted the regulation of HSPA8, and high expression levels of HSPA8 protein were detected in BC. HSPA8 is overexpressed in endometrial cancer to enhance the proliferative activity of cancer cells.³⁵ In addition, HSPA8 can enhance pancreatic cancer cell viability and inhibit the cytotoxicity of maslinic acid, thereby inhibiting

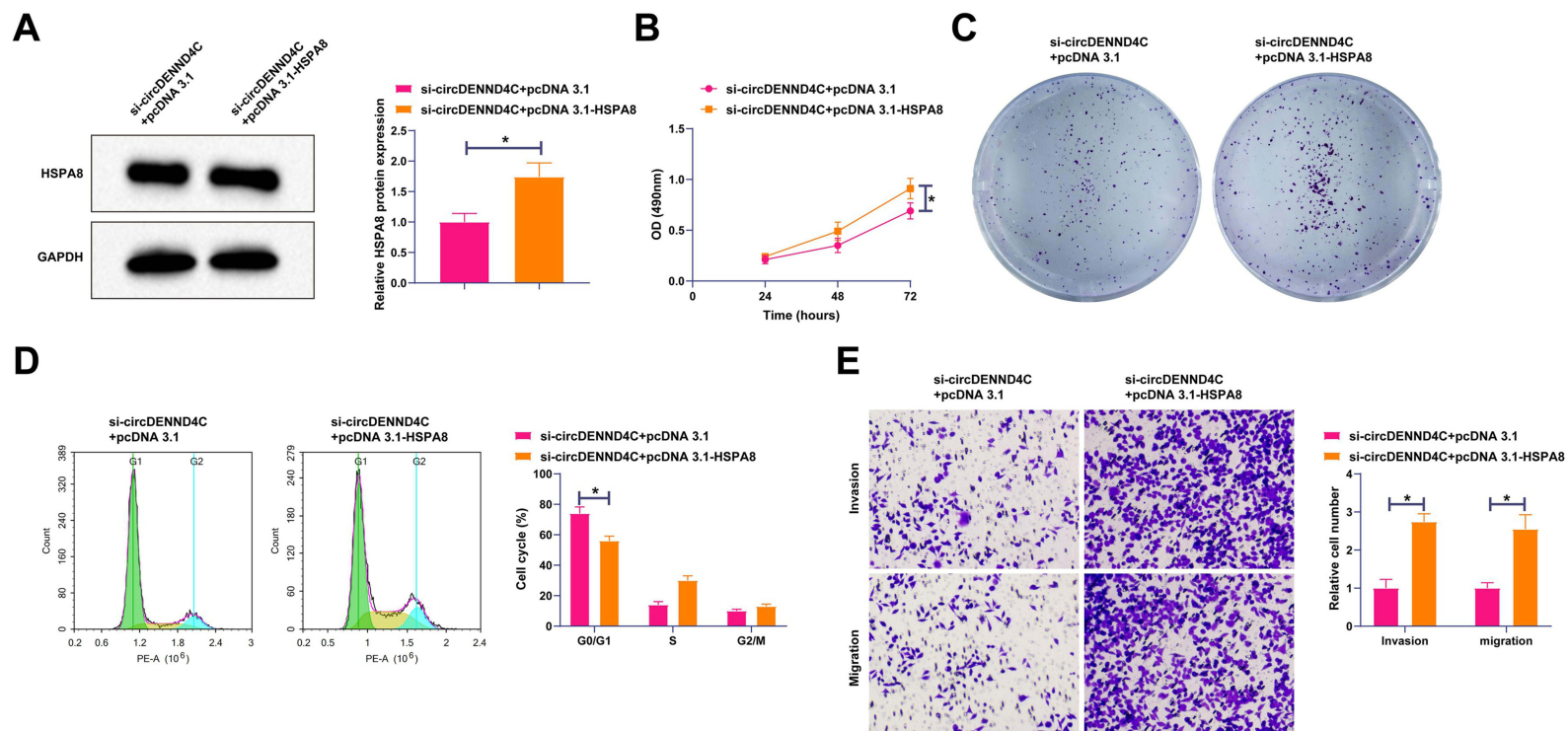


Figure 6 HSPA8 overexpression rescues the inhibitory effects of circDENND4C knockdown. MCF-7 cells were co-transfected with si-circDENND4C and a HSPA8 overexpression vector (pcDNA 3.1-HSPA8) or their respective controls. **(A)** Western blot analysis confirms that HSPA8 overexpression successfully restored its protein levels, which were suppressed by si-circDENND4C. **(B and C)** The anti-proliferative effects of circDENND4C knockdown, measured by MTT **(B)** and colony formation **(C)** assays, were reversed by HSPA8 overexpression. **(D)** HSPA8 overexpression abrogated the G0/G1 cell cycle arrest induced by circDENND4C silencing. **(E)** The suppression of cell migration and invasion following circDENND4C knockdown was rescued by the re-expression of HSPA8, as shown by Transwell assays. Data are expressed as mean \pm SD (N = 3). *P < 0.05.

autophagy and promoting the malignant progression of tumors.³⁶ Here, it was checked that elevating HSPA8 prohibited the suppressive effect of circDENND4C silencing on BC cells.

This study, while providing significant insights into the role of circDENND4C, miR-26a-5p, and HSPA8 in BC, encounters several limitations. The findings necessitate validation in a larger, more diverse cohort to enhance generalizability. Additionally, reliance on MCF-7 cell lines may not fully represent the heterogeneity of BC, and the predictive bioinformatics analyses require further experimental confirmation. The mechanistic pathways and the long-term impact of circDENND4C expression on survival also remain incompletely understood. A more detailed comprehension of the molecular mechanisms of BC can be achieved through comprehensive multi-center studies, expanded cell model systems, and improved methodological strategies.

Conclusion

The study concludes that circDENND4C is overexpressed in BC and has a connection to patient prognosis. In addition, circDENND4C competitively adsorbed miR-26a-5p to mediate HSPA8 expression, thus promoting BC in the normoxic environment. The data reveal new molecular targets for the formulation of BC-specific drugs or combination treatments.

Data Sharing Statement

The datasets used and/or analyzed during the present study are available from the corresponding author on reasonable request.

Ethics Approval and Consent to Participate

This study was approved by the ethical committees of Affiliated Hospital of Hebei Engineering University (Ethics approval number: 20141211HBEU). Written informed consent was provided by all patients prior to the study start. All procedures were performed in accordance with the ethical standards of the Institutional Review Board and The Declaration of Helsinki, and its later amendments or comparable ethical standards.

Funding

2019 Hebei Province Medical Science Research Project Plan (No.20190125); Medical Science Research Project of Hebei (No.20190961); Medical Science Research Project of Hebei (No.20200590).

Disclosure

The authors have no conflicts of interest to declare.

References

1. Harbeck N, Gnant M. Breast cancer. *Lancet*. 2017;389(10074):1134–1150. doi:10.1016/S0140-6736(16)31891-8
2. Chou J, Wang B, Zheng T, et al. MALAT1 induced migration and invasion of human breast cancer cells by competitively binding miR-1 with cdc42. *Biochem Biophys Res Commun*. 2016;472(1):262–269. doi:10.1016/j.bbrc.2016.02.102
3. Guarnerio J, Bezzi M, Jeong JC, et al. Oncogenic role of fusion-circRNAs derived from cancer-associated chromosomal translocations. *Cell*. 2016;165(2):289–302. doi:10.1016/j.cell.2016.03.020
4. Su M, Xiao Y, Ma J, et al. Circular RNAs in cancer: emerging functions in hallmarks, stemness, resistance and roles as potential biomarkers. *Mol Cancer*. 2019;18(1):90. doi:10.1186/s12943-019-1002-6
5. Li J, Sun D, Pu W, Wang J, Peng Y. Circular RNAs in cancer: biogenesis, function, and clinical significance. *Trends Cancer*. 2020;6(4):319–336. doi:10.1016/j.trecan.2020.01.012
6. Beilerli A, Gareev I, Beylerli O, et al. Circular RNAs as biomarkers and therapeutic targets in cancer. *Semi Cancer Biol*. 2022;83:242–252. doi:10.1016/j.semcancer.2020.12.026
7. Chen LL. The biogenesis and emerging roles of circular RNAs. *Nat Rev Mol Cell Biol*. 2016;17(4):205–211. doi:10.1038/nrm.2015.32
8. Jiang XM, Li ZL, Li JL, et al. A novel prognostic biomarker for cholangiocarcinoma: circRNA Cdr1as. *Eur Rev Med Pharmacol Sci*. 2018;22(2):365–371. doi:10.26355/eurrev_201801_14182
9. Wang X, Ji C, Hu J, et al. Hsa_circ_0005273 facilitates breast cancer tumorigenesis by regulating YAP1-hippo signaling pathway. *J Exp Clin Cancer Res*. 2021;40(1):29. doi:10.1186/s13046-021-01830-z
10. Wang L, Zhou Y, Jiang L, et al. CircWAC induces chemotherapeutic resistance in triple-negative breast cancer by targeting miR-142, upregulating WWP1 and activating the PI3K/AKT pathway. *Mol Cancer*. 2021;20(1):43. doi:10.1186/s12943-021-01332-8
11. Ren S, Liu J, Feng Y, et al. Knockdown of circDENND4C inhibits glycolysis, migration and invasion by up-regulating miR-200b/c in breast cancer under hypoxia. *J Exp Clin Cancer Res*. 2019;38(1):388. doi:10.1186/s13046-019-1398-2

12. Liu Y, Chen S, Zong ZH, Guan X, Zhao Y. CircRNA WHSC1 targets the miR-646/NPM1 pathway to promote the development of endometrial cancer. *J Cell Mol Med.* 2020;24(12):6898–6907. doi:10.1111/jcmm.15346
13. Kristensen LS, Jakobsen T, Hager H, Kjems J. The emerging roles of circRNAs in cancer and oncology. *Nat Rev Clin Oncol.* 2022;19(3):188–206. doi:10.1038/s41571-021-00585-y
14. Huang G, Liang M, Liu H, et al. CircRNA hsa_circRNA_104348 promotes hepatocellular carcinoma progression through modulating miR-187-3p/RTKN2 axis and activating Wnt/ β -catenin pathway. *Cell Death Dis.* 2020;11(12):1065. doi:10.1038/s41419-020-03276-1
15. Sang Y, Chen B, Song X, et al. circRNA_0025202 regulates tamoxifen sensitivity and tumor progression via regulating the miR-182-5p/FOXO3a axis in breast cancer. *Mol Ther.* 2019;27(9):1638–1652. doi:10.1016/j.ymthe.2019.05.011
16. Li J, Gao X, Zhang Z, et al. CircCD44 plays oncogenic roles in triple-negative breast cancer by modulating the miR-502-5p/KRAS and IGF2BP2/Myc axes. *Mol Cancer.* 2021;20(1):138. doi:10.1186/s12943-021-01444-1
17. Li PP, Li RG, Huang YQ, Lu JP, Zhang WJ, Wang ZY. LncRNA OTUD6B-AS1 promotes paclitaxel resistance in triple negative breast cancer by regulation of miR-26a-5p/MTDH pathway-mediated autophagy and genomic instability. *Aging.* 2021;13(21):24171–24191. doi:10.18632/aging.203672
18. Stricher F, Macri C, Ruff M, Muller S. HSPA8/HSC70 chaperone protein: structure, function, and chemical targeting. *Autophagy.* 2013;9(12):1937–1954. doi:10.4161/auto.26448
19. Zagouri F, Sergentanis TN, Gazouli M, et al. HSP90, HSPA8, HIF-1 alpha and HSP70-2 polymorphisms in breast cancer: a case-control study. *Mol Biol Rep.* 2012;39(12):10873–10879. doi:10.1007/s11033-012-1984-2
20. Veronesi U, Boyle P, Goldhirsch A, Orecchia R, Viale G. Breast cancer. *Lancet.* 2005;365(9472):1727–1741. doi:10.1016/S0140-6736(05)66546-4
21. Sun J, Li B, Shu C, Ma Q, Wang J. Functions and clinical significance of circular RNAs in glioma. *Mol Cancer.* 2020;19(1):34. doi:10.1186/s12943-019-1121-0
22. Long F, Lin Z, Li L, et al. Comprehensive landscape and future perspectives of circular RNAs in colorectal cancer. *Mol Cancer.* 2021;20(1):26. doi:10.1186/s12943-021-01318-6
23. Shan C, Zhang Y, Hao X, Gao J, Chen X, Wang K. Biogenesis, functions and clinical significance of circRNAs in gastric cancer. *Mol Cancer.* 2019;18(1):136. doi:10.1186/s12943-019-1069-0
24. Zheng X, Huang M, Xing L, et al. The circRNA circSEPT9 mediated by E2F1 and EIF4A3 facilitates the carcinogenesis and development of triple-negative breast cancer. *Mol Cancer.* 2020;19(1):73. doi:10.1186/s12943-020-01183-9
25. Ma D, Qin Y, Li S, et al. circDENND4C promotes proliferation and metastasis of lung cancer by upregulating BRD4 signaling pathway. *J Oncol.* 2021;2021:2469691. doi:10.1155/2021/2469691
26. Zhang ZJ, Zhang YH, Qin XJ, Wang YX, Fu J. Circular RNA circDENND4C facilitates proliferation, migration and glycolysis of colorectal cancer cells through miR-760/GLUT1 axis. *Eur Rev Med Pharmacol Sci.* 2020;24(5):2387–2400. doi:10.26355/eurrev_202003_20506
27. Maxmen A. Ebola outbreak declared an international public-health emergency. *Nature.* 2019. doi:10.1038/d41586-019-02221-3
28. Liang G, Liu Z, Tan L, Su AN, Jiang WG, Gong C. HIF1 α -associated circDENND4C promotes proliferation of breast cancer cells in hypoxic environment. *Anticancer Res.* 2017;37(8):4337–4343. doi:10.21873/anticancer.11827
29. Liu S, Yuan L, Li J, Liu Y, Wang H, Ren X. circDENND4C, a novel serum marker for epithelial ovarian cancer, acts as a tumor suppressor by downregulating miR-200b/c. *Ann Med.* 2023;55(1):908–919. doi:10.1080/07853890.2023.2185289
30. Beermann J, Piccoli MT, Viereck J, Thum T. Non-coding RNAs in development and disease: background, mechanisms, and therapeutic approaches. *Physiol Rev.* 2016;96(4):1297–1325. doi:10.1152/physrev.00041.2015
31. Qi X, Zhang DH, Wu N, Xiao JH, Wang X, Ma W. ceRNA in cancer: possible functions and clinical implications. *J Med Genet.* 2015;52(10):710–718. doi:10.1136/jmedgenet-2015-103334
32. Huang ZM, Ge HF, Yang CC, et al. MicroRNA-26a-5p inhibits breast cancer cell growth by suppressing RNF6 expression. *Kaohsiung J Med Sci.* 2019;35(8):467–473. doi:10.1002/kjm2.12085
33. Shi D, Wang H, Ding M, et al. MicroRNA-26a-5p inhibits proliferation, invasion and metastasis by repressing the expression of Wnt5a in papillary thyroid carcinoma. *Onco Targets Ther.* 2019;12:6605–6616. doi:10.2147/OTT.S205994
34. Wang Z, Liu T, Xue W, et al. ARNTL2 promotes pancreatic ductal adenocarcinoma progression through TGF/ β pathway and is regulated by miR-26a-5p. *Cell Death Dis.* 2020;11(8):692. doi:10.1038/s41419-020-02839-6
35. Shan N, Zhou W, Zhang S, Zhang Y. Identification of HSPA8 as a candidate biomarker for endometrial carcinoma by using iTRAQ-based proteomic analysis. *Onco Targets Ther.* 2016;9:2169–2179. doi:10.2147/OTT.S97983
36. Tian Y, Xu H, Farooq AA, et al. Maslinic acid induces autophagy by down-regulating HSPA8 in pancreatic cancer cells. *Phytother Res.* 2018;32(7):1320–1331. doi:10.1002/ptr.6064

Breast Cancer: Targets and Therapy

Publish your work in this journal

Breast Cancer - Targets and Therapy is an international, peer-reviewed open access journal focusing on breast cancer research, identification of therapeutic targets and the optimal use of preventative and integrated treatment interventions to achieve improved outcomes, enhanced survival and quality of life for the cancer patient. The manuscript management system is completely online and includes a very quick and fair peer-review system, which is all easy to use. Visit <http://www.dovepress.com/testimonials.php> to read real quotes from published authors.

Submit your manuscript here: <https://www.dovepress.com/breast-cancer—targets-and-therapy-journal>

Dovepress
Taylor & Francis Group